PRAMANA
— journal of
physics

Vol. 67, No. 5
November 2006
pp. 899–914

Nucleus–nucleus collisions at RHIC: A review

JEAN-YVES OLLITRAULT
Service de Physique Théorique, CEA Saclay, F-91191 Gif-sur-Yvette Cedex, France
E-mail: Jean-Yves.Ollitrault@cea.fr

Abstract. I review recent results from the heavy-ion programme at the Brookhaven Relativistic Heavy Ion Collider and their interpretation.

Keywords. Heavy-ion collisions; quark-gluon plasma.

PACS Nos 12.38.Mh; 24.10.Nz; 25.75.-q; 25.75.Ld; 25.75.Nq

1. Introduction

On April 18, 2005, a press release announced that a new state of matter had been discovered in ultrarelativistic nucleus–nucleus collisions at the relativistic heavy ion collider (RHIC) on Long Island, New York: not a gas of weakly interacting quarks and gluons as earlier expected, but something more like a liquid of strongly interacting quarks and gluons, with an extremely low viscosity. This claim was based on a consensus interpretation of experimental data by the four large detector groups, BRAHMS, PHENIX, PHOBOS and STAR [1].

In this talk, selected highlights from the RHIC programme are presented, with special emphasis on the most recent results, and on the developments which led to the press release. While significant discoveries have definitely been made at RHIC, I argue that a critical reassessement of the 'perfect liquid' scenario is necessary.

2. Theoretical approaches

The initial motivation for studying ultrarelativistic nucleus–nucleus collisions was to explore strong interactions at high temperature. The thermodynamics of QCD, the well-established theory of strong interactions, has been studied by a variety of methods. These studies led physicists to conjecture the phase diagram shown in figure 1 (left). This diagram has a rich structure at high baryon densities, where several phase transitions are expected due to colour superconductivity [4], which might eventually be observed in compact stars.

On the other hand, numerical results, based on lattice QCD calculations, are available only at small baryon densities. Fortunately, nucleus–nucleus collisions are

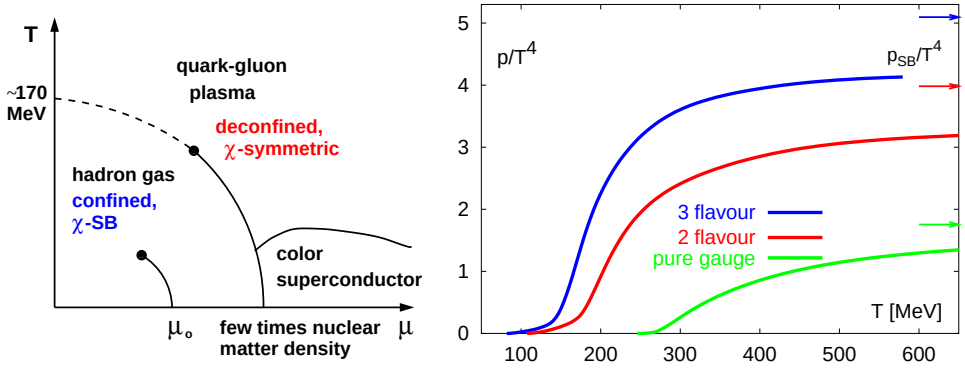

Figure 1. Left: Sketch of the QCD phase diagram [2]. Solid lines are first-order phase transitions and dots are critical points. The dotted line indicates a rapid, though continuous, transition between the low-temperature hadron phase and the high-temperature quark-gluon plasma. Right: Pressure P, as a function of the temperature, T, computed on the lattice for zero net baryon density (as many quarks as antiquarks) and various number of quark flavours [3]. P has been scaled by T^4 for dimensional reasons. Arrows indicate the values corresponding to non-interacting, massless quarks and gluons (Stefan's law for black-body radiation).

also expected to probe small baryon densities, for reasons to become clear below. At zero baryon density, lattice calculations clearly show a sharp structure in the equation of state (figure 1, right): the pressure increases by an order of magnitude in a narrow temperature interval around 170 MeV. This is interpreted as a transition from a hadron gas to a quark-gluon plasma. The transition is shown by lattice QCD to be continuous at zero baryon density, but it is generally expected to be first-order at higher baryon density, and the location of the critical point has been estimated on the lattice [5], although this is still a matter of debate [6].

The equation of state of QCD can also be calculated perturbatively. These calculations are only valid at asymptotically high temperatures, where the coupling constant is small. However, recent progress has been made recently in fixed-order calculations [7] and in resummation methods [8], and perturbative results are in agreement with lattice QCD down to temperatures of a few hundred MeV.

Although this is an exciting programme, which has an interest of its own, there is a gap between the thermodynamics of QCD and nucleus–nucleus collisions. A central gold–gold (Au–Au) collision at $\sqrt{s} = 200$ GeV per nucleon pair (the top RHIC energy) produces roughly 8000 particles. Due to the strong Lorentz contraction of the incoming nuclei, a high energy is deposited in a small volume: a back-of-the envelope calculation shows that the energy density is much larger than needed to produce a quark-gluon plasma. But the system expands into the vacuum as soon as it is produced: the crucial issue is whether interactions within the system are strong enough to achieve *local* thermodynamic equilibrium. If they are, it leaves us with the difficult task of finding signatures of QCD thermodynamics in a rapidly cooling system. This is the subject of the present talk.

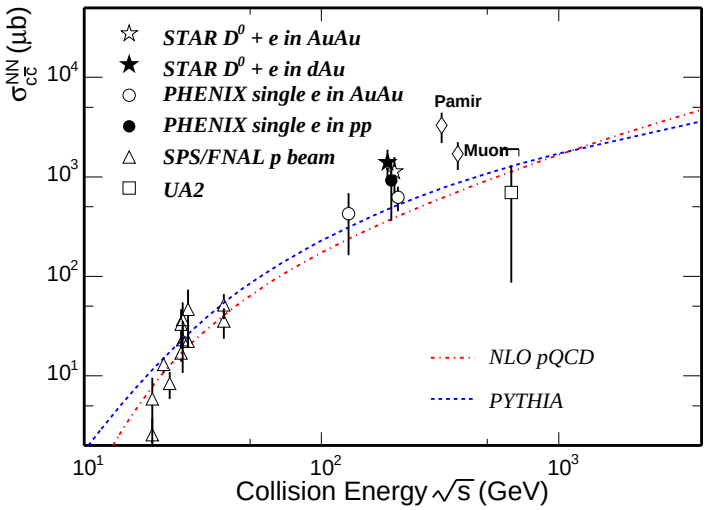

Figure 2. Cross-section for $c\bar{c}$ pair production [12] at various energies.

In recent years, a first-principles approach to high-energy QCD has been developed, the so-called 'color glass condensate' (CGC) [9]. This approach takes advantage of the fact that the density of partons at small Bjorken x is high, leading to the phenomenon of parton saturation, which can be studied by weak-coupling techniques. Although this method is better suited to electron–nucleus or proton–nucleus collisions [10], it has also been applied to nucleus–nucleus collisions [11]. As we shall see below, it sometimes provides an alternative explanation to the observed phenomena, without having recourse to a quark-gluon plasma, or to thermodynamics.

3. Particle yields

A lot of experimental activity is devoted to identify and count particles, and this has produced a wealth of interesting results.

3.1 *Open and hidden charm*

The production of $c\bar{c}$ quark–antiquark pairs is particularly interesting because it can be computed in perturbative QCD, and the production rate is much higher in a nucleus–nucleus collision than in an elementary collision. Preliminary results, shown in figure 2, are in agreement with next-to-leading order calculations in perturbative QCD.

Bound states of $c\bar{c}$ quarks, in particular J/ψ, deserve special interest: it was indeed predicted [13] that such bound states should disappear in a quark-gluon plasma due to screening of the colour charge, thus providing a unique signature of

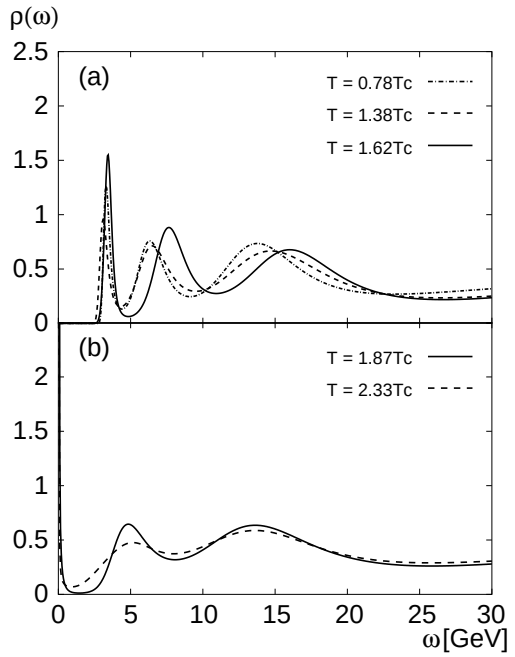

Figure 3. Mass spectrum of J/ψ for various values of the temperature T [14]. $T_{\rm c}$ denotes the transition temperature to the quark-gluon plasma. For T up to $1.62T_{\rm c}$, a clear peak is seen at the J/ψ mass, 3.6 GeV. The peak disappears at higher temperatures.

deconfinement. Twenty years after this early prediction, unfortunately, the theoretical picture is much more confused: lattice QCD calculations show that bound states do survive above the transition temperature to the quark-gluon plasma (figure 3). Furthermore, it has been realized that as the energy of the nucleus–nucleus collision increases, more and more $c\bar{c}$ pairs are produced per collision: a c and $\bar{c}$ from different pairs can recombine to form a J/ψ, thereby *increasing* the number of J/ψs [15].

The PHENIX Collaboration at RHIC has recently measured J/ψ production at RHIC. Results for nucleus–nucleus collisions are usually shown in terms of the nuclear modification factor, also known as R_{AA}, which we now define. The expected cross-section for a hard process in a nucleus–nucleus collision is the cross-section for the same process in a nucleon–nucleon collision, multiplied by the number of binary nucleon–nucleon collisions in a nucleus–nucleus collision. The number of binary collisions can easily be computed as a function of the impact parameter (or centrality) of the nucleus–nucleus collision. The nuclear modification factor R_{AA} of a given process is defined as the ratio of the observed rate, divided by the rate expected from binary-collision scaling. Please note that R_{AA} can only be measured if both nucleus–nucleus and proton–proton data are available.

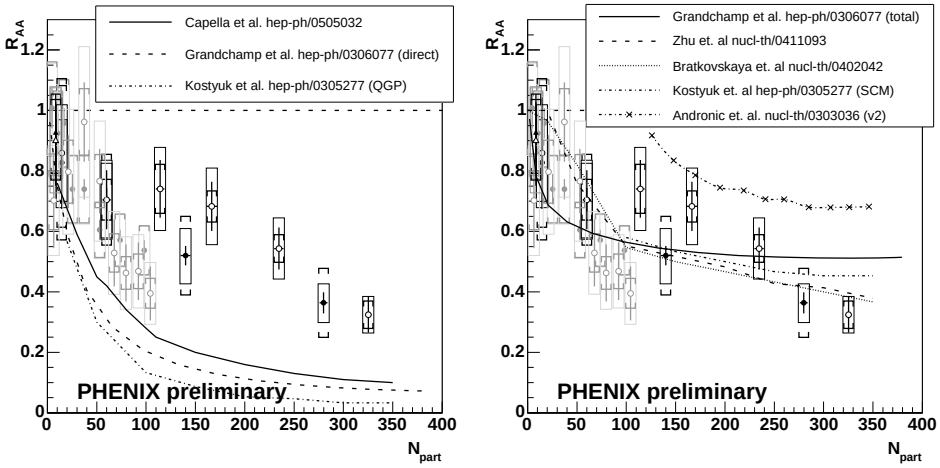

Figure 4. Nuclear modification factors (see text) for J/ψ production in Au–Au collisions [16], as a function of the number of nucleons participating in the collision, $N_{\rm part}$, which is used as an estimator of the centrality of the collision ($N_{\rm part}$ is largest for a central, head-on collision). Left: Compared with theoretical predictions without quark recombination. Right: Compared with theoretical predictions involving quark recombination from different pairs.

The R_{AA} for J/ψ production is shown in figure 4, together with various theoretical predictions. At lower energies (at the CERN SPS), R_{AA} for J/ψ was found to be smaller than 1. Various scenarios have been proposed to account for this 'suppression'. Extrapolation to RHIC energies produces the curves shown in figure 4, left. Although some suppression is clearly seen by PHENIX, it was overpredicted by the models. A better agreement was found when taking into account the recombination between c and $\bar{c}$ from different pairs (figure 4, right), although it cannot be considered as an evidence for recombination.

3.2 *Other hadrons*

So much for charm. What about the other hadrons, those made of light (u, d, s) quarks and antiquarks? Although fully non-perturbative, the situation is much simpler. All data are elegantly explained by statistical models: particle numbers are computed in a grand-canonical ensemble, where the temperature T and the baryon chemical potential μ_b are fitted to reproduce measured particle ratios. As can be seen in figure 5, fits are of very good quality. This 'thermal' behaviour is in fact observed over a wide range of colliding energies in heavy-ion collisions. A compilation of results is displayed in figure 6. The leftmost points correspond to RHIC data. The baryon chemical potential is very small at RHIC: the 8000 produced particles, with zero net baryon number, overwhelm the 394 incoming baryons in a central Au–Au collision. More interestingly, the temperature is very close to the temperature of the transition to the quark-gluon plasma, as computed

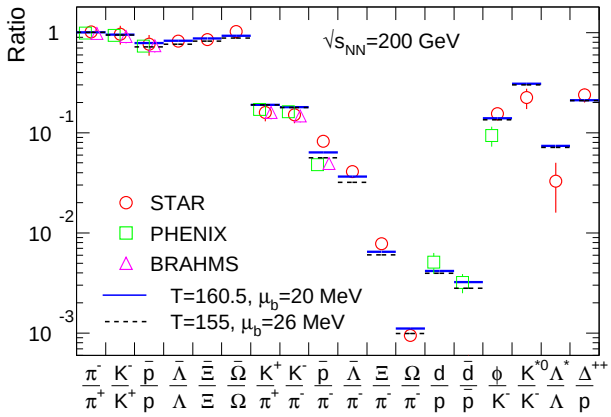

Figure 5. Thermal fits to measured particle ratios [17].

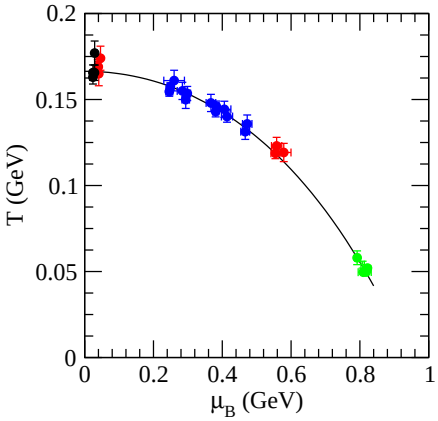

Figure 6. Thermal fit parameters for heavy-ion collisions at RHIC, SPS, AGS, SIS (from left to right) [18]. The solid line is a polynomial fit.

in lattice QCD. This is interpreted as evidence that a quark-gluon plasma has been formed, which then hadronizes.

One can object that similar fits to particle ratios measured in $p\bar{p}$ [19] or even e^+e^- [20] collisions yield exactly the same temperature. The difference, however, is that statistical models overpredict abundances of strange hadrons in elementary collisions, and a third parameter (the strangeness suppression factor) must be introduced to account for this effect. In nucleus–nucleus collisions, even strangeness equilibrates. But even this is not a compelling evidence for quark-gluon plasma formation: it has recently been shown that the colour glass condensate picture also predicts strangeness equilibration, without having recourse to statistical models [21]. The success of statistical models is in fact a puzzle for theorists, because thermal fits are done using hadron masses in the vacuum; now, at temperatures as high as 160 MeV, medium effects are expected to have a big influence on hadron masses, in particular as a consequence of chiral symmetry restoration.

4. Single-particle distributions: Soft particles

More detailed information on the collision dynamics can be inferred from the momentum distributions of identified particles. Rapidity spectra (the rapidity is related to the velocity v_z along the collision axis by $v_z = \tanh y$) are narrower in nucleus–nucleus collisions than in proton–proton collisions (at the same energy per nucleon), showing substantial nuclear stopping up to the top RHIC energy. The data shown below are obtained near midrapidity, where most of the detailed analyses are carried out.

4.1 *Transverse collective flow*

In proton–proton collisions, proton–nucleus, or even deuteron–nucleus collision, transverse momentum (p_{T}) distributions are thermal, as particle ratios. This means that the p_{T} distribution at zero rapidity is well-described by a Boltzmann factor (neglecting the effects of quantum statistics, which are small in practice):

$$\frac{\mathrm{d}N}{\mathrm{d}y\mathrm{d}^2p_{\mathrm{T}}} \propto \exp\left(-\frac{m_{\mathrm{T}}}{T}\right), \tag{1}$$

where $m_{\mathrm{T}} \equiv \sqrt{p_{\mathrm{T}}^2 + m^2}$ and the parameter T has the same value for all particles (figure 7, left). This exponential spectrum applies to the soft sector only (p_{T} below 2 GeV). Spectra become flatter at higher momenta, reflecting the transition from the exponential behaviour to the perturbative, power-law behaviour.

The situation is qualitatively different in nucleus–nucleus collisions where heavier particle spectra are significantly flatter at low m_{T} (figure 7, right). This is the first hint of the phenomenon called 'collective flow', which is expected if the matter produced in the nucleus–nucleus collision reaches local thermodynamic equilibrium. It then behaves like a fluid, whose pressure decreases gradually to zero from the center of the fireball to the outside vacuum. The pressure gradient accelerates the fluid outwards ($\mathrm{d}\vec{v}/\mathrm{d}t \propto -\vec{\nabla}P$). The fluid velocity boosts the thermal distribution, and eq. (1) is replaced with [23]

$$\frac{\mathrm{d}N}{\mathrm{d}y\mathrm{d}^2p_{\mathrm{T}}} \propto \exp\left(-\frac{\gamma m_{\mathrm{T}} - \gamma v p_{\mathrm{T}}}{T}\right), \tag{2}$$

where v is the fluid velocity and $\gamma = 1/\sqrt{1-v^2}$ is the associated Lorentz factor. This simple ansatz, with proper refinements, is called a blast-wave parametrization. It gives a very good description of p_{T} spectra of identified hadrons with $p_{\mathrm{T}} < 2$ GeV/c [24].

4.2 *Elliptic flow*

A specific feature of nucleus–nucleus collisions is that one can measure the azimuthal angle of particles, ϕ, with respect to the impact parameter of the collision

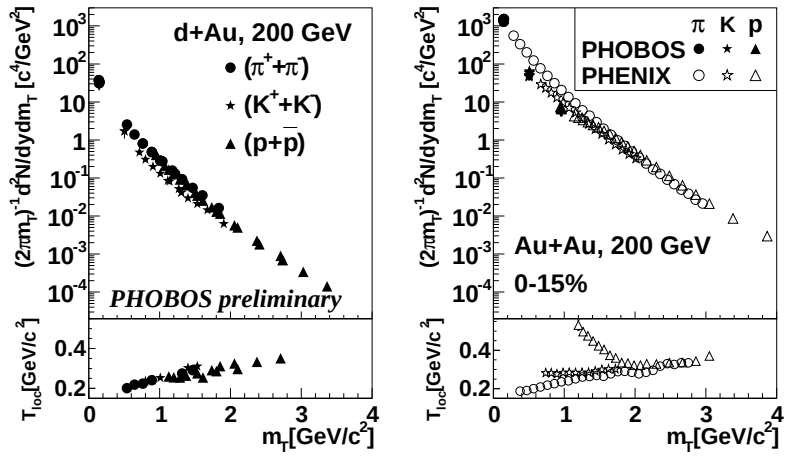

Figure 7. Transverse mass spectra in deuteron–gold (left) and gold–gold (right) collisions, in logarithmic scale [22]. $T_{\rm loc}$ is the inverse of the local slope of the spectrum, which is independent of $m_{\rm T}$ for an exponential (thermal) spectrum.

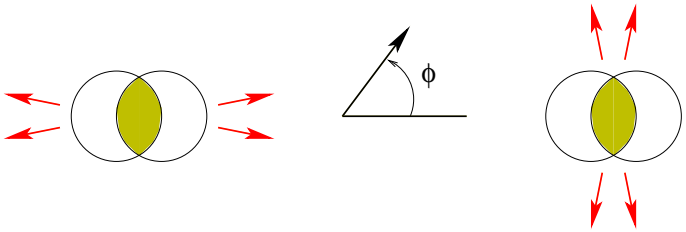

Figure 8. Nucleus–nucleus collision viewed in the plane perpendicular to the collision axis (transverse plane). The azimuthal angle ϕ of a particle is measured from the direction of impact parameter. Arrows indicate preferred directions of emission in the case of positive (left) or negative (right) elliptic flow.

(see figure 8). The initial particle production is isotropic in ϕ, since elementary parton–parton collisions occur on a much shorter transverse scale than the impact parameter of the nucleus–nucleus collision. Anisotropies in the ϕ distribution, also known as 'anisotropic flow', are thus thought to be sensitive probes of subsequent (also known as secondary, final-state) interactions among the produced particles. Anisotropic flow is characterized by the coefficients v_n of the Fourier expansion of the ϕ distribution:

$$\frac{{\rm d}N}{{\rm d}\phi} = \frac{N}{2\pi}\left(1 + 2v_1\cos\phi + 2v_2\cos 2\phi + \cdots\right). \tag{3}$$

The most important term in this expansion is v_2, also known as elliptic flow. When two nuclei collide with non-zero impact parameter, the overlap region, where particle creation occurs, has the shape of an almond, shown as a shaded area in

figure 8. Pressure gradients are largest along the smaller axis of the almond. As a consequence, the fluid velocity is also largest along this axis, and in the end there are more particles with transverse momenta parallel to the impact parameter than perpendicular. This results in positive v_2.

Although positive elliptic flow had long been predicted [25] and observed at lower energies [26], its large magnitude at RHIC was a big surprise to many people in the field. For the first time, it was as large as predicted by ideal-fluid models, which assume local thermodynamic equilibrium. This is illustrated in figure 9 which shows model calculations together with experimental data. Although the agreement is not perfect, both the magnitude and the qualitative features are well-reproduced. One aspect which has received particular attention is the strong mass ordering of v_2: when comparing different particles at the same transverse momentum p_{T}, heavier particles have smaller v_2. As we shortly explain, this is clear evidence not only of collective flow, but also of relativistic collective flow, in the sense that the flow velocity is a significant fraction of the velocity of light.

When elliptic flow is present, the fluid velocity v depends on the orientation ϕ. We write this dependence in the form

$$\gamma(\phi)v(\phi) = \gamma_0 v_0 + 2u_2 \cos 2\phi. \tag{4}$$

To a good approximation, particles follow the fluid, so that ϕ of the particle is that of the fluid. The azimuthal distribution of particles with a given p_{T} is then obtained by inserting eq. (4) in eq. (2). (Recall that d^2p_{T} in the left-hand side of eq. (2) stands for $p_{\mathrm{T}}\mathrm{d}p_{\mathrm{T}}\mathrm{d}\phi$.) Expanding to leading order in u_2, using the identity $\mathrm{d}\gamma = v\,\mathrm{d}(\gamma v)$, and identifying with eq. (3), one obtains

$$v_2(p_{\mathrm{T}}) = \frac{u_2}{T}\,(p_{\mathrm{T}} - v_0 m_{\mathrm{T}})\,. \tag{5}$$

A more careful calculation [28] shows that this expression is valid only if p_{T} is large enough. Equation (5) explains most of the qualitative features seen in figure 9: the linear increase of v_2 with p_{T} for pions, for which $m_{\mathrm{T}} \simeq p_{\mathrm{T}}$; the mass ordering of v_2, since $m_{\mathrm{T}} \equiv \sqrt{p_{\mathrm{T}}^2 + m^2}$ is larger for heavier particles at a given p_{T}. Clearly, the mass ordering is strong only if the fluid velocity, v_0, is large enough. Best fits to data give $v_0 \simeq 0.7$ for semicentral Au–Au collisions at RHIC [24].

The elliptic flow of charmed hadrons was recently estimated indirectly through their decay electrons. It was expected that the charmed quark, which is heavy, would be harder to deviate from its trajectory than a light quark [29], and therefore would exhibit less elliptic flow. The v_2 of charm has been estimated theoretically as a function of a diffusion coefficient, which might be calculable on the lattice [30]. Preliminary data, shown in figure 10 together with model calculations, suggest that the elliptic flow of charmed hadrons follow the general trend: it is smaller at a given p_{T} than for lighter hadrons, but not significantly smaller than predicted by the above mass ordering.

4.3 *How perfect is the RHIC liquid?*

Let us briefly explain the arguments for the 'perfect liquid'. Elliptic flow plays an important part: it is as large as predicted by ideal-fluid models. To understand what

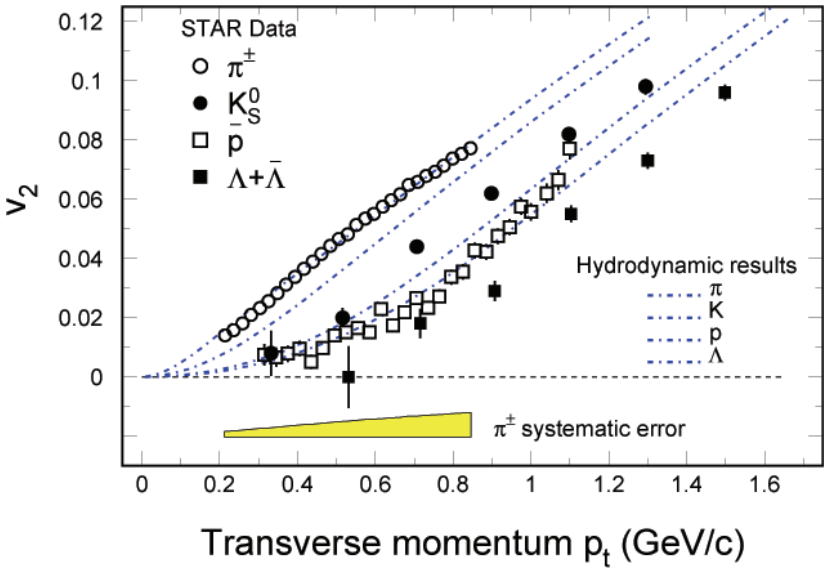

Figure 9. Elliptic flow of identified particles as a function of their transverse momentum, compared with ideal-fluid calculations [27].

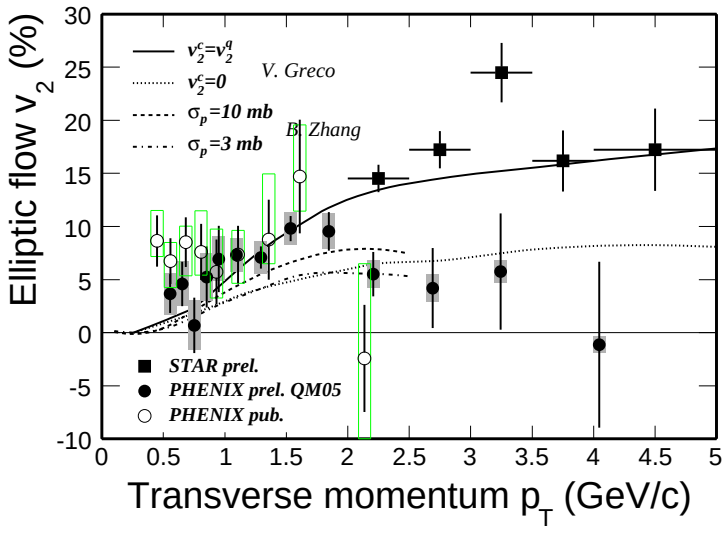

Figure 10. Charm elliptic flow [12].

this means in terms of particle physics, one can solve a Boltzmann equation (which is known to converge towards ideal-fluid dynamics when the number of collisions is large) and see what cross-sections are needed to reproduce ideal hydrodynamics. Claims were made that partonic cross-sections as large as 47 mb were needed. This, in turn, suggested that the viscosity of the quark-gluon plasma was extremely low;

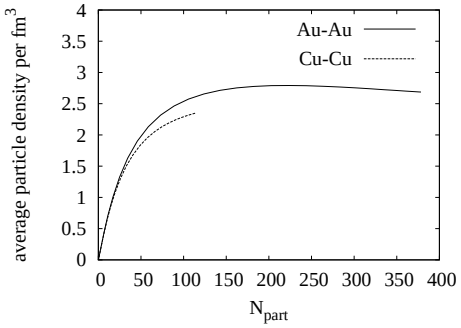

Figure 11. Average particle density in the fireball at the time when elliptic flow builds up, as a function of the number of participant nucleons (see figure 4), for Au–Au and Cu–Cu collisions.

now, that the viscosity can be computed analytically in supersymmetric gauge theories using the AdS/CFT correspondence, and it turns out to be extremely low [32]: this was an unexpected bridge between string theory and nuclear physics.

In spite of the press release, most experts now agree that in order to reproduce the detailed features of the data, large viscous corrections are needed [33] and there has been a lot of activity lately on viscous relativistic hydrodynamics [34]. It has been shown that early hydrodynamic calculations underestimated elliptic flow [35]. Numerical solutions of the Boltzmann equation may also require some revision as they do not seem to converge towards ideal hydrodynamics [31].

Instead of going into technical details, I prefer to show figure 11, which will help the reader make his own mind what we see at RHIC. This plot shows the average particle density in the fireball at the time when elliptic flow appears in the system [36]. This density is defined as the ratio of the observed particle number to the volume of the system at that time (which, for dimensional reasons, scales as the transverse size). Except for very peripheral collisions, this density is remarkably constant, in the range of 2–3 fm^{-3}: since the size of a hadron is of the order of 1 fm, we are clearly dealing with a dense liquid, which cannot be described by conventional hadronic physics. I believe that quantitative estimates of the viscosity and of the equation of state at this density should be available soon.

5. Single-particle distributions: Hard particles

The colliding energy at RHIC is large enough to produce particles with transverse momenta up to 15 GeV/c. Compared to the previous heavy-ion programmes at the CERN SPS, this opens up a new physics window. Hard particles are produced in hard interactions, which can be described perturbatively. A convenient observable to characterize hard processes in nucleus–nucleus collisions is the nuclear modification factor R_{AA} defined in §3.1, which equals 1 if the cross-section scales with the number of binary collisions, as expected in perturbative QCD.

The photons created in hard collisions between quarks of the incoming nuclei do not interact after they have been produced: one expects no nuclear modification

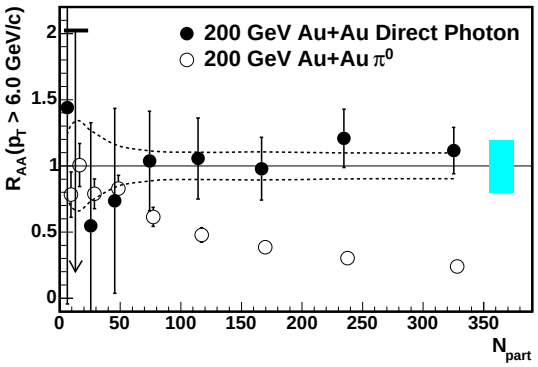

Figure 12. Nuclear modification factors (see text) for hard photons and neutral pions [37] in Au–Au collisions, as a function of the number of participants (see figure 4).

for these so-called direct photons. This is confirmed by the recent measurements shown in figure 12, which show that $R_{AA} = 1$ within error bars for all centralities.

By contrast, neutral pions in the same p_{T} range are more and more suppressed as the collision becomes more central, by a factor up to 5 for the most central collisions! The reason is simple: hard pions come from the fragmentation of a quark or gluon jet. Unlike photons, quarks and gluons interact with the nuclear medium. One expects that they lose energy as they go through a quark-gluon plasma. This phenomenon, called jet quenching, has been extensively studied [38], and the suppression of high-p_{T} neutral pions is understood as a direct consequence of jet quenching (see also §7 below). Other baryons and mesons show a comparable amount of suppression. The energy lost by jets, as inferred from the suppression of high-p_{T} particles, is so large that the observed high-p_{T} particles are those coming from the surface, which do not travel through the quark-gluon plasma. This, in turn, means that they are not very sensitive to the energy loss itself [39].

The energy loss is expected to be smaller for quark jets than for gluon jets. Now, quark jets can be tagged using hadrons containing a c or a b quark, since heavy flavours are produced in hard processes. On this basis, heavy-flavoured mesons were predicted to be less suppressed at high p_{T} than light mesons [40]. Furthermore, the energy loss is predicted to be smaller for b than for c quarks, and B mesons, carrying a b quark, can be seen through their semileptonic decays: most electrons with $p_{\mathrm{T}} > 5$ GeV/c are expected to originate from B mesons [41]. Preliminary measurements, however, suggest that the suppression is also large for heavy flavours, and definitely larger than would have been expected from b quark decays (figure 13).

6. Single-particle distributions: Between soft and hard

Interesting phenomena occur in the intermediate p_{T} range between the soft and hard sectors studied in §§4 and 5. For $2 < p_{\mathrm{T}} < 3$ GeV/c, one finds as many protons as positive pions at mid-rapidity in central Au–Au collisions [42], while

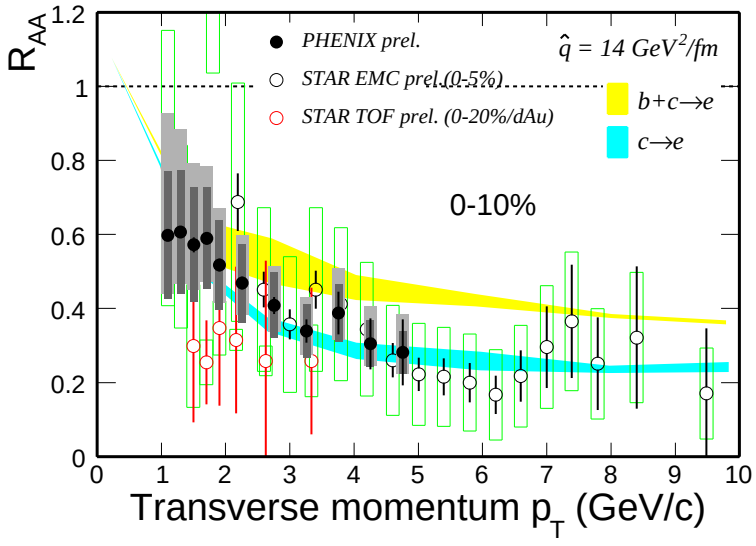

Figure 13. Heavy-flavour production at high p_{T} [12].

there are three times less ps than π^+s in p–p collisions. Another anomaly is found in elliptic flow, which violates the mass ordering explained in §4: v_2 is significantly larger for protons than for pions (figure 14). The same anomaly is seen for strange baryons [44], whose v_2 is larger than mesons in the intermediate momentum range. A popular interpretation of these peculiarities is that baryons (respectively mesons) are formed in the quark-gluon plasma by the coalescence of three quarks (resp. a quark and an antiquark) [45]. One then finds that the underlying v_2 of the quark is the same for mesons and baryons (figure 14).

7. Correlations

It is impossible to reconstruct jets in nucleus–nucleus collisions at RHIC due to the large background formed by the thousands of emitted particles. In §5, we explained how the energy loss of jets can be inferred from leading, hard particles. A more direct information about the jet structure is provided by azimuthal correlations between hard particles (figure 15). The di-jet structure is clearly seen as two peaks at $\Delta\phi = 0$ (when both trigger particle and associated particle belong to the same jet) and at $\Delta\phi = \pi$ (when the trigger particle and the associated particle belong to jets moving in opposite directions). While the height and width of the near-side peak remain constant, the away-side peak becomes smaller and smaller as the collision becomes more central. This again reflects the phenomenon of jet quenching: hard particles can only be emitted near the surface, thus particles belonging to the same jet do not lose energy. On the other hand, the particles in the opposite jet must make their way through the medium before they reach the detector and lose a lot of energy.

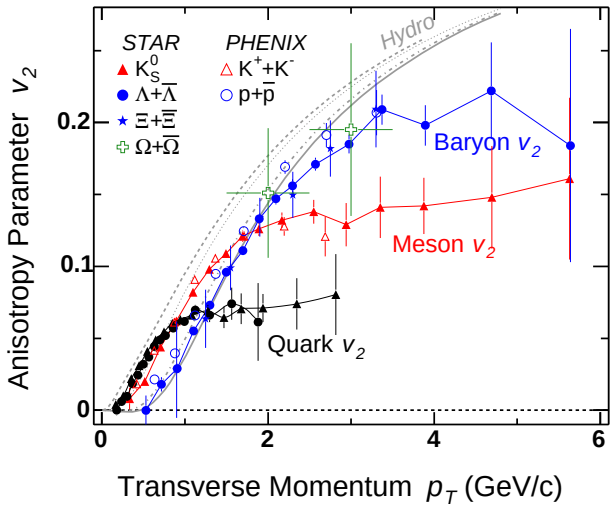

Figure 14. Elliptic flow of baryons and mesons in the intermediate p_T range [43]. The 'quark v_2' is obtained by scaling down the diagram by a factor 2 for mesons, and 3 for baryons.

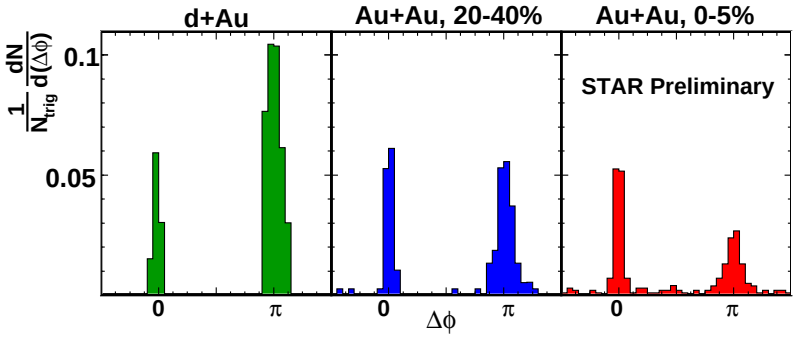

Figure 15. Azimuthal correlations between hard particles [46]: for each particle with p_T between 8 and 15 GeV/c ('trigger' particle) one counts the number of particles $p_T > 6$ GeV/c, at a given azimuthal angle $\Delta\phi$ relative to the trigger particle ('associated' particles).

8. Conclusions

Most of the physics we see at RHIC is new. All the phenomena discussed above, in particular elliptic flow and high-p_T suppression due to jet quenching, had been predicted long ago, and they were seen as soon as RHIC started: the first data clearly showed a medium opaque to high-energy quarks and gluons, behaving collectively like a fluid moving outwards at 70% the velocity of light.

Detailed analyses, however, require high statistics, and many essential results appeared only in 2005: quite unexpectedly, charm appears to behave like light flavours, in that it displays strong collectivity, and high-p_T suppression. The first

detailed results on J/ψ suppression at RHIC are now available, and they hint at interesting new physics. Di-jets are seen for the first time in heavy-ion collisions, with essentially no background.

Experiment is ahead of theory at RHIC, but theory is rapidly catching up. Although data on high-p_{T} suppression are globally in quantitative agreement with predictions of non-Abelian energy loss models, some of the new data are still challenging. The RHIC liquid is not that perfect, and viscous corrections are being carefully estimated.

References

[1] BRAHMS Collaboration: I Arsene *et al*, *Nucl. Phys.* **A757**, 1 (2005)
PHOBOS Collaboration: B B Back *et al*, *Nucl. Phys.* **A757**, 28 (2005)
STAR Collaboration: J Adams *et al*, *Nucl. Phys.* **A757**, 102 (2005)
PHENIX Collaboration: K Adcox *et al*, *Nucl. Phys.* **A757**, 184 (2005)
[2] F Karsch, hep-lat/0601013
[3] F Karsch, E Laermann and A Peikert, *Phys. Lett.* **B478**, 447 (2000)
[4] M G Alford, K Rajagopal and F Wilczek, *Phys. Lett.* **B422**, 247 (1998)
D H Rischke, *Prog. Part. Nucl. Phys.* **52**, 197 (2004)
M G Alford, C Kouvaris and K Rajagopal, *Phys. Rev. Lett.* **92**, 222001 (2004)
[5] Z Fodor and S D Katz, *J. High Energy Phys.* **0404**, 050 (2004)
[6] Rajiv V Gavai, *Pramana – J. Phys.* **67**, 885 (2006)
[7] A Vuorinen, *Phys. Rev.* **D67**, 074032 (2003)
[8] J P Blaizot, E Iancu and A Rebhan, hep-ph/0303185
[9] E Iancu and R Venugopalan, arXiv:hep-ph/0303204
[10] J P Blaizot, F Gelis and R Venugopalan, *Nucl. Phys.* **A743**, 13 (2004); *Nucl. Phys.* **A743**, 57 (2004)
[11] A Krasnitz, Y Nara and R Venugopalan, *Phys. Rev. Lett.* **87**, 192302 (2001)
[12] X Dong, *Nucl. Phys.* **A774**, 343 (2006)
[13] T Matsui and H Satz, *Phys. Lett.* **B178**, 416 (1986)
[14] M Asakawa and T Hatsuda, *Phys. Rev. Lett.* **92**, 012001 (2004)
[15] P Braun-Munzinger and J Stachel, *Phys. Lett.* **B490**, 196 (2000)
[16] PHENIX Collaboration: H Pereira Da Costa, *Nucl. Phys.* **A774**, 747 (2006)
[17] A Andronic, P Braun-Munzinger and J Stachel, *Nucl. Phys.* **A772**, 167 (2006)
[18] J Cleymans, H Oeschler, K Redlich and S Wheaton, *Phys. Rev.* **C73**, 034905 (2006)
[19] F Becattini and U W Heinz, *Z. Phys.* **C76**, 269 (1997); Erratum, *ibid.* **C76**, 578 (1997)
[20] F Becattini, *Z. Phys.* **C69**, 485 (1996)
[21] F Gelis, K Kajantie and T Lappi, *Phys. Rev. Lett.* **96**, 032304 (2006)
[22] A Trzupek *et al*, *Nucl. Phys.* **A774**, 469 (2006)
[23] K S Lee, U W Heinz and E Schnedermann, *Z. Phys.* **C48**, 525 (1990)
[24] F Retiere and M A Lisa, *Phys. Rev.* **C70**, 044907 (2004)
[25] J Y Ollitrault, *Phys. Rev.* **D46**, 229 (1992)
[26] NA49 Collaboration: C Alt *et al*, *Phys. Rev.* **C68**, 034903 (2003)
[27] STAR Collaboration: J Adams *et al*, *Phys. Rev.* **C72**, 014904 (2005)
[28] N Borghini and J Y Ollitrault, nucl-th/0506045
[29] G D Moore and D Teaney, *Phys. Rev.* **C71**, 064904 (2005)
[30] P Petreczky and D Teaney, *Phys. Rev.* **D73**, 014508 (2006)
[31] D Molnar and P Huovinen, *Phys. Rev. Lett.* **94**, 012302 (2005)

[32] P Kovtun, D T Son and A O Starinets, *Phys. Rev. Lett.* **94**, 111601 (2005)
[33] D Teaney, *Phys. Rev.* **C68**, 034913 (2003)
[34] U W Heinz, H Song and A K Chaudhuri, *Phys. Rev.* **C73**, 034904 (2006)
R Baier, P Romatschke and U A Wiedemann, *Phys. Rev.* **C73**, 064903 (2006)
[35] T Hirano, U W Heinz, D Kharzeev, R Lacey and Y Nara, *Phys. Lett.* **B636**, 299 (2006)
[36] R S Bhalerao, J P Blaizot, N Borghini and J Y Ollitrault, *Phys. Lett.* **B627**, 49 (2005)
[37] PHENIX Collaboration: S S Adler *et al*, *Phys. Rev. Lett.* **94**, 232301 (2005)
[38] R Baier, Y L Dokshitzer, A H Mueller and D Schiff, *J. High Energy Phys.* **0109**, 033 (2001)
M Gyulassy, I Vitev, X N Wang and B W Zhang, arXiv:nucl-th/0302077
C A Salgado and U A Wiedemann, *Phys. Rev. Lett.* **89**, 092303 (2002)
[39] K J Eskola, H Honkanen, C A Salgado and U A Wiedemann, *Nucl. Phys.* **A747**, 511 (2005)
[40] N Armesto, A Dainese, C A Salgado and U A Wiedemann, *Phys. Rev.* **D71**, 054027 (2005)
[41] M Djordjevic, M Gyulassy, R Vogt and S Wicks, *Phys. Lett.* **B632**, 81 (2006)
[42] BRAHMS Collaboration: E J Kim, *Nucl. Phys.* **A774**, 493 (2006)
[43] P Sorensen, *Acta Phys. Hung.* **A24**, 221 (2005)
[44] STAR Collaboration: J Adams *et al*, *Phys. Rev. Lett.* **95**, 122301 (2005)
[45] D Molnar and S A Voloshin, *Phys. Rev. Lett.* **91**, 092301 (2003)
[46] STAR Collaboration: D Magestro, *Nucl. Phys.* **A774**, 573 (2006)